JOURNAL OF MATERIALS SCIENCE 26 (1991) 5644–5654

Hydrogen effects in a dual-phase microalloy steel

T. ALP*, F. I. ISKANDERANI, A. H. ZAHED
Chemical and Materials Engineering Department, King Abdulaziz University, PO Box 9027, Jeddah 21413, Saudi Arabia

A dual-phase steel containing niobium, vanadium and titanium as microalloying elements was tested for hydrogen embrittlement (HE). The susceptibility to HE was observed to be closely related to the microstructural state. Hydrogenated specimens intercritically annealed at relatively low temperatures to develop martensite islands in a ferrite matrix basically exhibited quasi-cleavage fracture with some ductile dimpling. The mode of fracture in charged specimens quenched from higher intercritical annealing temperatures was predominantly intergranular fracture along prior austenite grain boundaries and cracking of martensite laths. The detrimental role of residual stresses, retained austenite and microalloying carbides in the process of HE is discussed.

1. Introduction

The technological significance of the development and wide spread application of microalloyed steels with low carbon content cannot be overemphasized. Research in the last two decades, in particular, has clearly demonstrated the fact that minor additions of metals such as niobium, vanadium and titanium coupled with a novel approach to thermomechanical processing results in steels considerably stronger and tougher than the plain carbon steels which they have replaced. This important achievement has been made possible through the beneficial influences of grain refinement on the strength and toughness, and a correct appreciation of the ways whereby fine grain sizes could be produced.

During controlled rolling of microalloyed high-strength low-alloy steels (HSLA), with decreasing temperature carbides and carbo-nitrides of niobium, vanadium and titanium begin to precipitate in austenite, often on preferred sites such as grain boundaries, sub-boundaries and dislocation networks. This may profoundly influence recovery and recrystallization and exercise a strong inhibitive effect on austenite grain growth. During the course of austenite transformation to ferrite, carbide precipitates can effectively govern the transformation rate and the morphology of ferrite. When hot working is continued in the ferrite state a fine dispersion of these carbides may retard or even suppress recrystallization. The resulting grain refinement, yielding very small grains with an average grain size typically around 10 μm together with fine dispersions of carbide or carbo-nitrides, contributes to the development of high strength.

The principal microalloying elements, niobium, vanadium and titanium, form highly stable face-centred cubic carbides and nitrides. The solubility products computed by Norberg and Aronson [1] and Narita [2] as a function of temperature for the carbides and nitrides of these metals evidently indicate that the carbides possess higher solubilities than their respective nitrides. Consequently those species such as VC with higher solubilities in austenite at high temperatures will form upon cooling a larger volume fraction of precipitate and give rise to significant precipitation strengthening. On the other hand the relatively less readily soluble NbC is a more potent grain-growth inhibitor than VC.

More often than not the microalloying elements in steel form carbides and nitrides which have substantial mutual solubility. Using the atom probe microanalysis technique, Dunlup and Turner [3] confirmed this fact while examining a vanadium–titanium microalloy steel. Scanning transmission electron microscope (STEM) microanalysis has been used to demonstrate that the composition of the precipitate varies over wide limits with changes in temperatures [4]. The kinetics of precipitate coarsening is significantly governed by the solubility. This, in turn, determines the effectiveness of grain boundary and dislocation pinning by precipitate particles. Titanium carbide, on the other hand, is observed to coarsen much more slowly in austenite than vanadium carbide. Investigations on vanadium carbide and nitride dispersions in alpha-iron have demonstrated conclusively that the rate of coarsening is markedly decreased with the successive replacement of carbon by nitrogen in the precipitates [5]. Similar observations have been made [6] when

* *Present address*: Manchester Materials Science Centre, UMIST, Manchester, UK.

0022–2461/91 $03.00 + .12

the vanadium in the precipitate is partially substituted with titanium. The solubilities of precipitates in ferrite are considerably lower than in austenite.

For effective pinning of grain boundaries and subboundaries [7–9] by precipitates the following three conditions must be satisfied. The particle size and spacing must not exceed critical values, the volume fraction of precipitate must be sufficient to maintain critical spacing, and finally, the rates of precipitate coarsening must remain low. Accordingly, bearing in mind the solubility of the various precipitates, with a sufficient amount of microalloying elements and carbon together with nitrogen to meet the prerequisite stoichometric ratio, maximum solubility at the highest processing temperature should be aimed at. During γ–α transformation in microalloyed steels, the presence of strong carbide-forming elements and the low carbon content result in very fine alloy carbide dispersions which may normally be revealed by transmission electron microscope (TEM) investigations. In these steels, precipitation during the transformation is observed to take place primarily at the γ–α interfaces. Generally the observed morphology may either appear as periodic banded arrays of fine oriented particles [10, 11] (interphase precipitation), or fine alloy carbide fibres with their growth direction normal to the interface [12] (fibrous carbides). A small variation in temperature during transformation can suppress interphase precipitation and permit fibrous carbides to grow. Thus slowing down the γ–α reaction rate may favour fibrous growth [13]. For more detailed information on the various aspects of HSLA steels the reader may be referred to Gray *et al.* [14] and De Ardo [15].

The role of microstructure in the hydrogen embrittlement (HE) of steel has been investigated by several researchers [16–19]. In recent years it has become increasingly clear that microstructural control through thermomechanical processing and chemical composition does provide a spectrum of responses to embrittling media. HE has been shown to depend characteristically on both temperature and strain rate, which suggests that hydrogen transport is required by the embrittlement mechanism. Around room temperature where embrittlement is experienced, comparative diffusivity data [20, 21] imply that hydrogen transport is impeded by interactions with a number of lattice defects which are assumed to act as trapping sites for hydrogen. Oriani [22] considered the possibility of multiple trapping sites for hydrogen in steel, including but not limited to dislocations, internal interfaces and microcracks. Although hydrogen–defect interaction has been investigated by several experimental techniques [21, 23, 24], trapping data obtained hitherto tend to be of a qualitative nature. This is certainly attributable to the complex effects of numerous variables on the susceptibility to embrittlement. Refinement of grain size [25], homogeneously distributed fine particles of TiC [26] and titanium atoms in ferrite [27] could lead to benign trapping of hydrogen. Accordingly, high non-equilibrium concentrations of hydrogen are innocuously held at certain traps which prevent or delay hydrogen build-up at potential fracture nucleation sites, thus mitigating embrittlement.

The trap theory of HE due to Pressouyre [28] basically assumes that a crack will initiate on a given defect if the concentration of trapped hydrogen exceeds a certain critical value specific to the defect considered. Although the conclusions deduced from the theory are generally dependent upon the initial state of the material, and more specifically on trap characteristics, hydrogen transport mode and hydrogen localization, it is suggested that a rationalized thermomechanical treatment could yield an adequate trap density and morphology to control embrittlement.

Dual-phase steels are a relatively new class of HSLA steels characterized by a microstructure consisting of a dispersion of hard martensite islands in a soft, ductile matrix of ferrite. These steels typically possess low proof strength and high ultimate tensile strength (UTS) compared to conventional, low-carbon formable steels. They display high work-hardening rates in the early phase of plastic deformation, and substantial ductility during cold work relative to their strength in the formed state. These characteristics are directly related to their microstructural state [29–31].

The conventional method for the production of these steels involves isothermal annealing in the intercritical ($\gamma + \alpha$) phase region followed by quenching to convert the austenite to martensite. In practice, full conversion of austenite to martensite is almost never accomplished, and consequently other microstructural constituents result. In particular, during intercritical annealing the old ferrite may experience a "back-growth" into the austenite to form new epitaxial ferrite in the early stages of cooling. Furthermore, pearlite or bainite may form prior to or instead of completion of austenite transformation of any remaining austenite to martensite. Some austenite in the form of fine particles too small to transform to martensite may be retained in the dual-phase structure. The relative proportions of these numerous microstructural constituents which coexist after quenching is determined by the composition of the austenite at the intercritical annealing temperature (ICT) and the quenching rate therefrom. More detailed information on the physical metallurgy of dual-phase steels may be found in Kot and Morris [31].

The purpose of the present paper is to present the findings of some experimental investigations recently carried out by the authors on the mechanical properties and the susceptibility to HE of a dual-phase treated microalloyed steel.

2. Methods and materials

Flat dumb-bell shaped tensile test specimens (Fig. 1) were machined with their long axis parallel to the rolling direction of a 1 mm thick strip rolled from a block of pipeline steel supplied by British Steel, Swindon Laboratory, Sheffield, UK. The steel had the chemical composition shown in Table I.

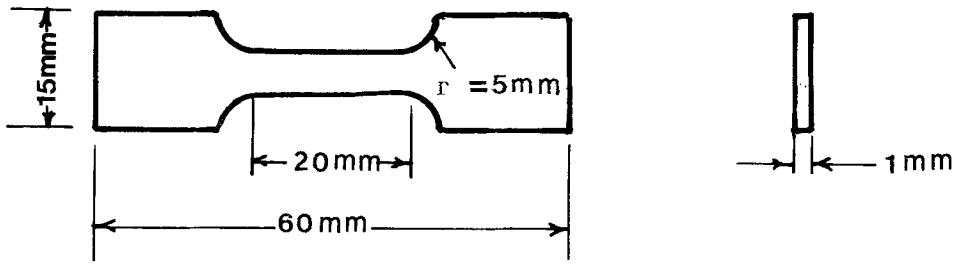

Figure 1 Geometry of tensile test specimens.

TABLE I The chemical composition of × 65 steel (wt %)

C	Mn	V	Nb	Ti	Si	S	P	Cr	Co	Cu	Al	Sn	Ni	As
0.05	1.4	0.06	0.04	0.01	0.2	0.006	0.017	0.01	0.01	0.32	0.042	0.01	0.25	0.0001

2.1. Dual-phase heat treatment

Machined tensile test pieces were intercritically annealed in an inert atmosphere for 20 min to permit phase equilibration to take place at a predetermined temperature. The specimens were then rapidly quenched into a well-stirred ice–water mixture. A set of intercritical annealing temperatures in the range 749–900 °C was chosen to prepare groups of specimens with different ferrite/martensite ratios.

2.2. Hydrogenation

Specimens polished and ground to 0.25 μm surface finish were degreased in methanol, dried and etched for 15 s in 2% Nital solution prior to hydrogenation. Specimens were electrolytically charged with hydrogen for 30 min at a current density of 10 mA cm^{-2} in 0.4 M sulphuric acid solution poisoned with 5 mg l^{-1} of arseneous trioxide.

For standardization, all hydrogenated specimens were subjected to uniaxial tensile stress after a fixed time interval of 5 min from the end of hydrogen charging. Mechanical tests were carried out using an Instron universal machine model 1190 at a constant crosshead speed of 2 mm min^{-1}. The mechanical behaviour of specimens was characterized by recording load–displacement curves, and noting the elongation at fracture.

Optical microscopy and scanning electron fractography were employed to study flat and fracture surfaces, respectively. Representative areas and inclusions/precipitates were analysed quantitatively using the energy-dispersive (EDAX) technique in conjunction with a Philips 505 scanning electron microscope.

3. Results

3.1. Microstructure and mode of fracture in unhydrogenated dual-phase steel

Optical metallography and electron fractography were employed to study the salient structural characteristics resulting from dual-phase heat treatments and prominent fractographic features associated with hydrogen effects. The mechanical behaviour of unhydrogenated and hydrogenated material is interpreted in the light of these observations and the current theories of HE.

The microstructure of the steel as received consisted primarily of equiaxed ferrite grains, with small regions of unresolved pearlite lying along the grain boundaries and occasionally extending towards the interior of the grains. Hot rolling of this material resulted in the usual textured microstructure of elongated ferrite grains and discontinuous pearlite stringers parallel to the rolling direction.

The detailed microstructure of the dual-phase treated steel exhibited a marked dependence on the intercritical annealing temperature and the rate of cooling. Relatively lower annealing temperatures and cooling rates gave rise to dual-phase microstructures essentially consisting of martensite islands in ferrite. Fig. 2 depicts a typical dual-phase structure produced by intercritical annealing at 749 °C and subsequent water quenching to 0 °C. Etching in an aqueous solution of boiling alkaline chromate stains the martensite black, the old (primary) ferrite grey and the epitaxial ferrite formed during intercritical annealing white.

Irrespective of the intercritical annealing temperature, all specimens in the uncharged state predominantly exhibited a ductile mode of transgranular

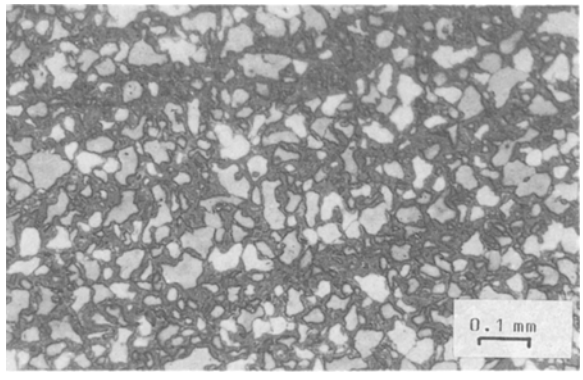

Figure 2 Dual-phase microstructure produced by intercritical annealing at 749 °C and water-quenching to 0 °C. The surface is etched in boiling chromate solution to reveal martensite (dark background), old ferrite (grey), and new epitaxial ferrite (white).

fracture chracterized by extensive dimpling in the entire cross-section. Fig. 3 shows typical microvoid coalescence in the fracture surface of an uncharged specimen intercritically annealed at 749 °C. With increasing annealing temperature microvoids become progressively smaller. Fig. 4 illustrates a selected area exhibiting a fracture surface with evidently finer dimples observed in specimens quenched from 900 °C. A small amount of localized quasi-cleavage which recurs in all uncharged specimens increases perceptibly with increasing annealing temperature. The fracture surfaces of uncharged specimens were free from secondary cracks. Non-metallic inclusions were not detected under the scanning electron microscope. Careful examination of flat surfaces did not reveal any surface cracks.

Martensite morphology is principally governed by the annealing temperature and quenching rate. Intermediate temperatures together with moderately high cooling rates yield ostensibly larger martensite islands embedded in ferrite matrix, as depicted in Fig. 5. A cold solution of 2% Nital etches martensite light grey. Stepping up the intercritical annealing temperature above ~ 830 °C brings about a fundamental change in martensite morphology such that martensite islands are replaced by martensite laths.

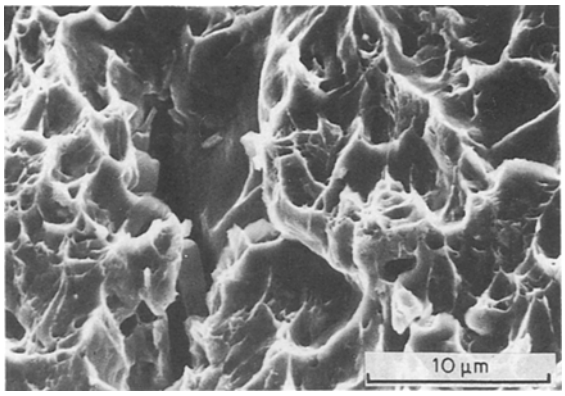

Figure 3 Extensive microvoid coalescence manifested in the fracture surface of a specimen intercritically annealed at 749 °C and water-quenched to 0°C.

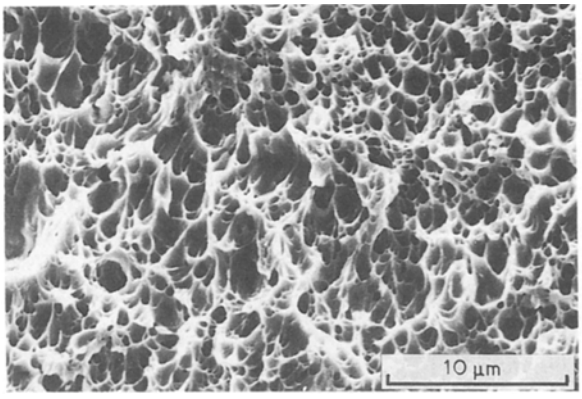

Figure 4 Fine dimples in a specimen intercritically annealed at 900 °C.

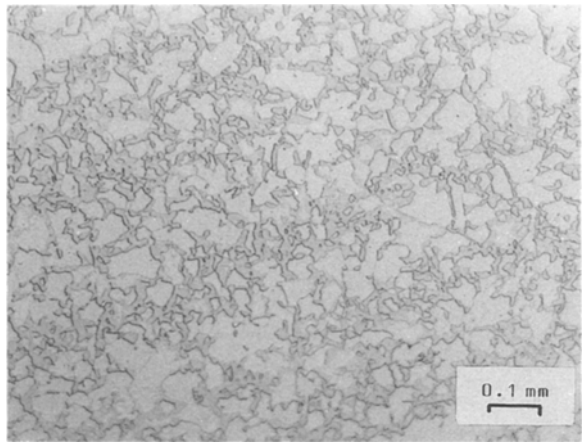

Figure 5 Martensite islands (light grey) in a specimen quenched from 783 °C (Nital etch).

3.2 Effect of hydrogenation on the mode of fracture

Hydrogenation greatly alters the mode of fracture and its detailed characteristics. Charged specimens exhibit progressively reduced ductility with increasing intercritical annealing temperatures. Specimens having a dual-phase structure consisting of hard martensite islands engulfed in soft ferrite matrix essentially manifest a mixed mode of fracture characterized by quasi-cleavage (Fig. 6) and the usual ductile dimpling. The relative proportion of the two features is primarily determined by the mechanical characteristics and the relative amounts of the microstructural constituents resulting from a given dual-phase heat treatment. Nevertheless, irrespective of the relative quantities of the phases and their respective morphologies, hydrogenation causes a tremendous loss of tensile ductility.

With the coarsening of martensite islands in specimens quenched from intermediate annealing temperatures around 800 °C, HE becomes most pronounced. The limited extent of fine dimpling associated with low residual tensile ductility (less than 1%) is confined to certain locations in the ferritic matrix which simultaneously displays quasi-cleavage. As indicated in Fig. 7, the appearance of secondary cracks represents a tendency for a mixed mode of fracture. As martensite morphology undergoes a transition from "island" type

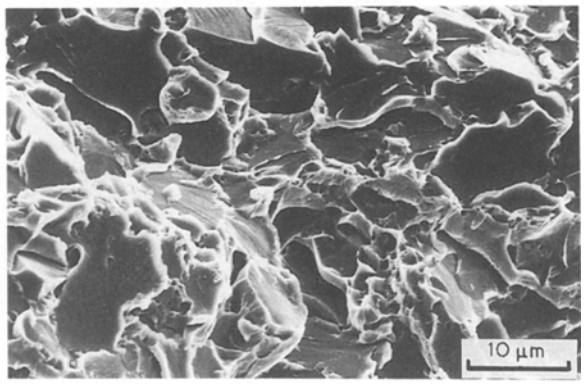

Figure 6 Predominantly quasi-cleavage region in a hydrogenated dual-phase steel intercritically annealed at 749 °C.

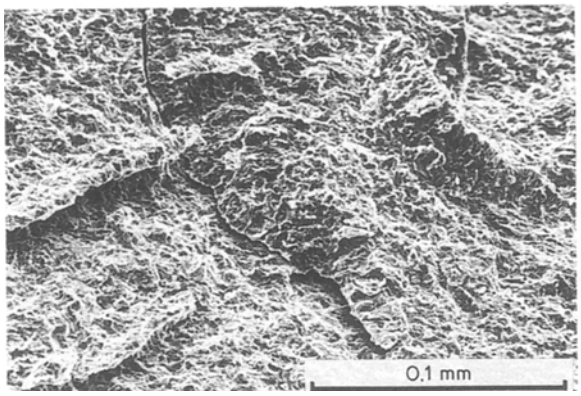

Figure 7 Mixed mode of fracture in a dual-phase steel quenched from 783 °C.

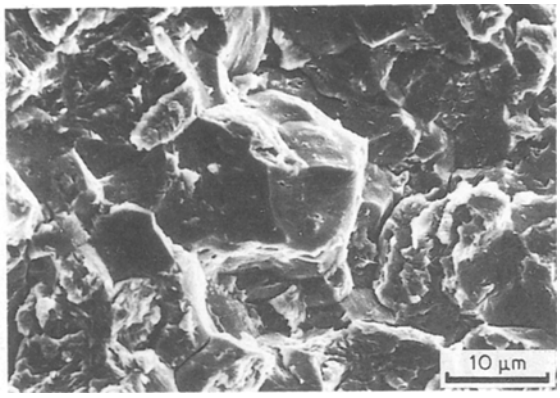

Figure 10 Grain-boundary separation and cleavage fracture in a hydrogenated specimen quenched from 900 °C.

to "lath" type with increasing intercritical annealing temperature, the mode of fracture in hydrogenated specimens changes from a combination of dimpled quasi-cleavage (Fig. 8) to a predominantly intergranular fracture with the dimpling in a small volume fraction of ferrite enveloping prior austenite grains (Fig. 9). Fracture in specimens charged with hydrogen following austenitization at 900 °C occurs in a predominantly brittle intergranular mode (Fig. 10). A small amount of fine dimpling is indicative of residual ductility. The measured elongation in this case is less than unity.

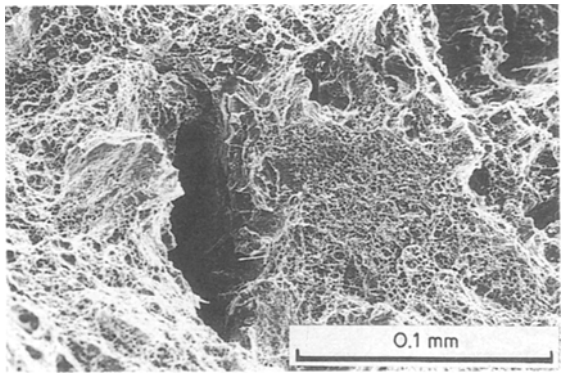

Figure 8 Mixed mode of fracture consisting of quasi-cleavage facets and fine dimples in a hydrogenated specimen intercritically annealed at 853 °C.

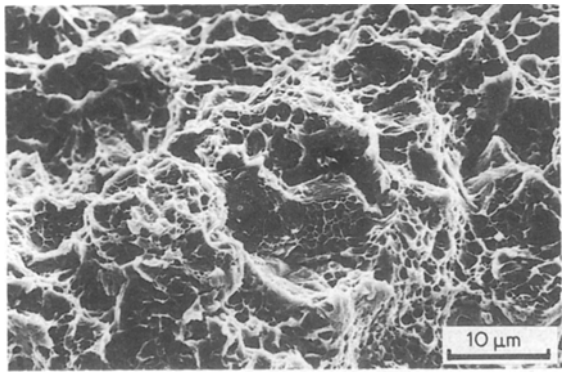

Figure 9 Mixed mode of fracture characterized by localized regions of fine dimples, quasi-cleavage and intergranular fracture in a hydrogenated specimen quenched from 870 °C.

Examination by optical microscopy of flat surfaces unhydrogenated and hydrogenated along the gauge length, before and after tensile testing, revealed significant evidence pertaining to the hydrogen-induced cracking (HIC) mechanism in this steel. While uncharged specimens were observed to be completely free from any kind of microcracks or surface irregularities, surfaces examined after hydrogenation displayed, irrespective of the microstructural state, embryonic cracks nucleated at various initiation sites (Fig. 11). During the course of tensile stressing these minute embryonic cracks continue to grow until they link up to form a continuous crack path generally parallel to the direction of rolling (Fig. 12). In contrast, the crack path in hydrogen-charged specimens containing lath martensite is comparatively more tortuous.

3.3. Hydrogenation, microstructure, mechanical behaviour interrelation

The as-received material, which had a largely ferritic microstructure with about 3.7 wt % of fine pearlite, was characterized by a clearly defined yield point at a stress level of 500 MPa. The maximum elastic strain was 5%. The ultimate tensile strength was noted to be 640 MPa with an associated uniform elongation of 16.5%. Rupture occurs at a nominal fracture stress of 440 MPa when the total elongation is about 29%. Charging this material with hydrogen decreases the yield strength and ultimate tensile strength to 487 and 618 MPa, respectively. The nominal stress–strain curves for the as-received material before and after charging with hydrogen are given in Fig. 13.

The uncharged and charged mechanical behaviour of dual-phase treated steel specimens is governed by the microstructural state, which is related to intercritical annealing variables (annealing temperature and time allowed for phase equilibration) and the subsequent quenching rate. In the present investigations, increasing the annealing temperature, while keeping the annealing time constant, resulted in a progressive increase of strength and decrease of tensile ductility (Fig. 14). This behaviour is directly related to the relative proportion of phases emanating from

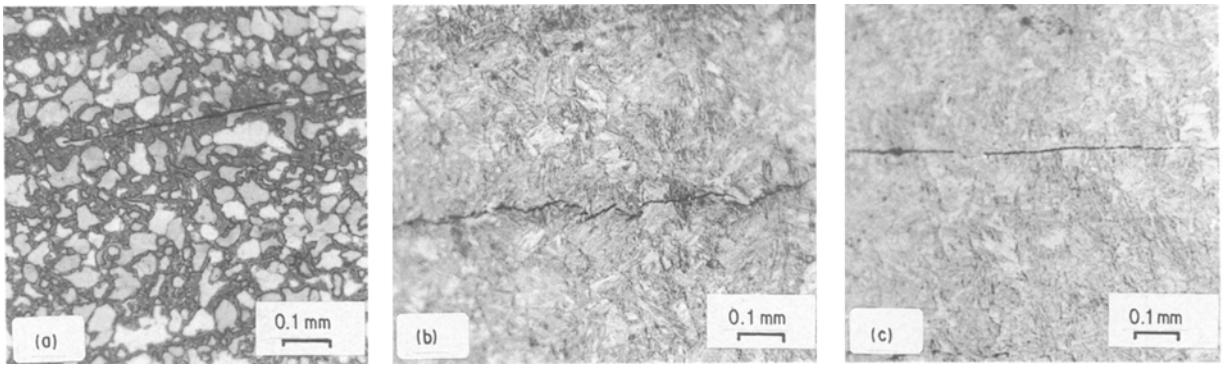

Figure 11 Embryonic hydrogen-induced cracks initiated at (a) ferrite–martensite interface, (b) lath martensite and (c) alloy carbide precipitates.

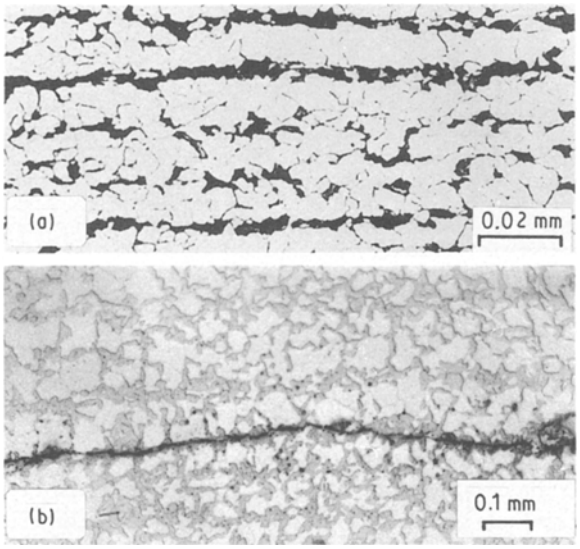

Figure 12 (a) Texture of pearlite stringers (black phase) and elongated ferrite (white phase) developed after hot rolling; (b) hydrogen-induced crack propagating preferentially in ferrite between martensite islands and parallel to rolling direction during tensile stressing. Nital etch.

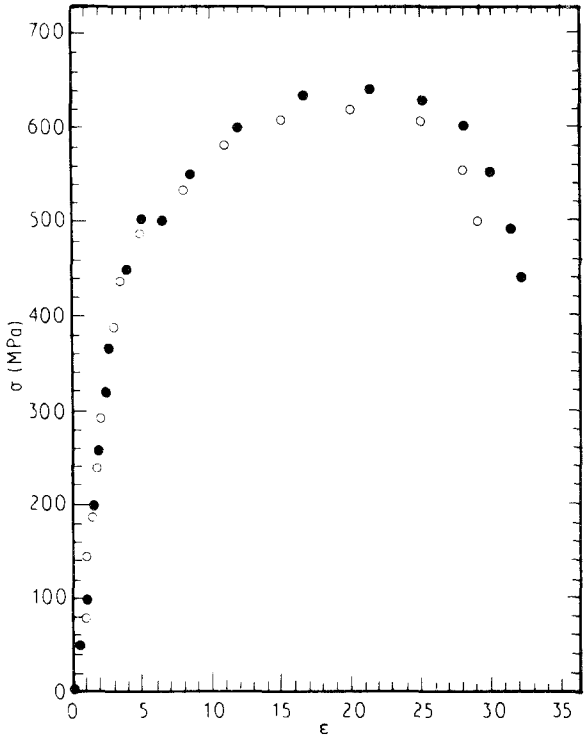

Figure 13 Nominal stress–strain curves for the as received steel (●) before and (○) after hydrogenation.

dual-phase heat treatment. Most importantly, increasing the annealing temperature increases the volume fraction of martensite which contributes most strikingly to the development of strength and reduction of ductility. Fig. 15 shows the variation of the volume fraction of martensite with ICT.

The influence of microstructure on the mechanical behaviour of dual-phase steel specimens charged with hydrogen is reflected in the stress–strain plots presented in Fig. 16. Irrespective of the intercritical annealing temperature, hydrogenation decreases the strength and tensile ductility of dual-phase steel drastically. Fig. 16 indicates the charged mechanical behaviour of specimens annealed at different temperatures. The mode of fracture in hydrogenated specimens is predominantly brittle, with a certain amount of residual ductility which is governed by the relative proportion of the microstructural constituents present.

The stress–strain curves of charged specimens are characterized by continuous yielding, absence of strength maxima, absence of clear necking and much reduced elongation at fracture. Careful examination of fracture surfaces did not reveal any obvious fracture initiation sites. Non-metallic inclusions and alloy carbides were absent from the scene of fracture. The fine carbide precipitates encountered on grain facets (Fig. 10) did not play an obvious role in the crack nucleation process.

Three factors in the plastic deformation process of dual-phase steels are of particular interest in relation to HE. Firstly, in the initial stage of deformation, rapid work-hardening is accompanied by a rapid build-up of back stresses generated by the plastic incompatibility of ferrite and martensite. Secondly, in the intermediate stage of work-hardening, which involves up to about 4% strain, transformation of retained austenite to martensite occurs. Finally, in the third stage (4–18% strain) immobile dislocation cell

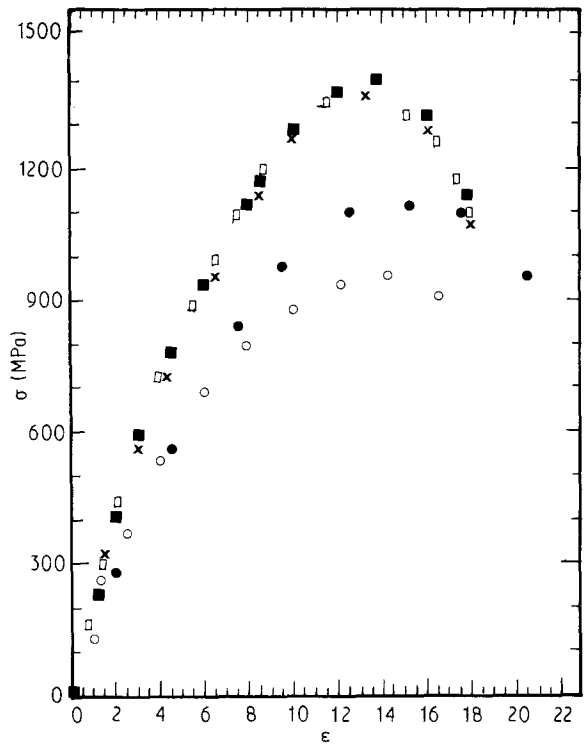

Figure 14 The mechanical behaviour of dual-phase steel specimens resulting from intercritical annealing at (○) 749, (●) 783, (×) 853, (■) 870 and (□) 902 °C.

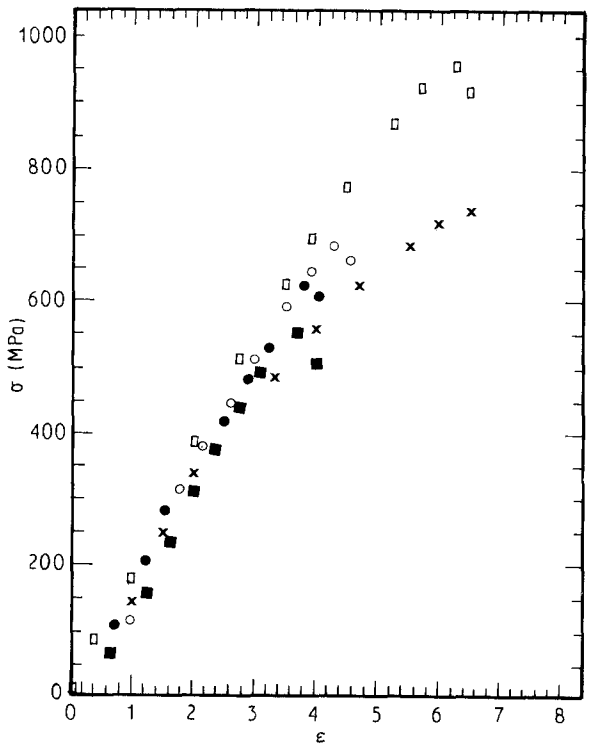

Figure 16 Mechanical behaviour of hydrogenated dual-phase steel specimens intercritically annealed at (×) 749, (●) 783, (□) 853, (○) 878 and (■) 900 °C.

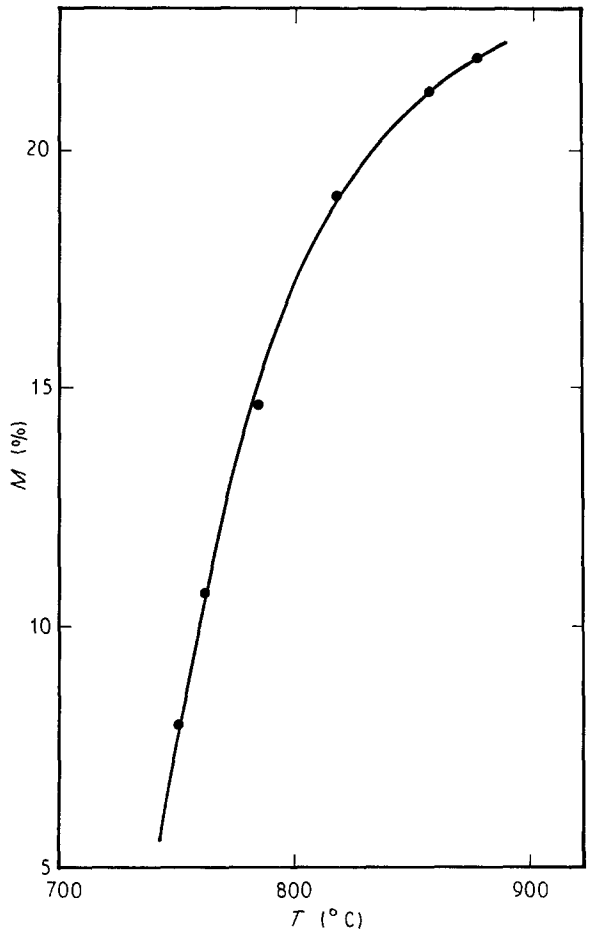

Figure 15 Variation of volume fraction of martensite, M, with ICT.

structures form when additional deformation in ferrite is dictated by dynamic recovery and cross-slip and by ultimate yielding of martensite [32]. Furthermore, since the formation of martensite as a result of dual-phase heat treatment and the transformation of retained austenite is accompanied by a positive volume change, the surrounding ferrite experiences substantial residual stresses. Thus, vast incoherent interfaces around martensite islands (or martensite laths) in a highly strained ferrite matrix provide strong traps for hydrogen. Therefore, Oriani's suggestion [33] that hydrogen precipitates at locations of high elastic stress is consistent with the cleavage mode of fracture observed in largely ferritic specimens (Fig. 6) and intergranular failure in the martensitic structures (Fig. 10). As Fig. 16 indicates, charged specimens fail prematurely when the nominal strain is typically in the range of 4–6%, corresponding to the beginning of the last stage of work-hardening for the uncharged material. It is at this stage that retained austenite has already transformed to martensite, and the hydrogen concentration at triaxially stressed regions attains the critical values to cause interface decohesioning.

Fig. 17 shows the variation of the maximum obtainable strength (UTS or the breaking strength for specimens failing before necking), σ, as a function of annealing temperature. The strength passes through a minimum for specimens containing large proportions of ferrite and retained austenite, and attains a maximum around 850 °C when the microstructure consists essentially of ferrite and lath martensite with some retained austenite. At relatively low temperatures dispersions of niobium, vanadium and titanium carbides are known to exist in the matrix. Titanium carbide has been shown to play a beneficial role in mitigating HE in a low-carbon manganese HSLA steel [34] when TiC particles are semi-coherent and finely dispersed.

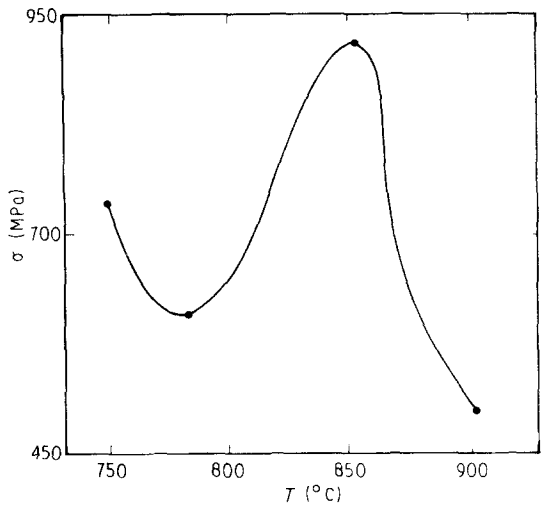

Figure 17 Variation of maximum strength with intercritical annealing temperature for hydrogenated dual-phase steel.

Computations made from solubility product equations [35, 36] show that VC totally dissolves in austenite between 800 and 850 °C, while only about 17% Nb goes into solution at 900 °C. The dissolution of VC and a part of NbC, which act as injurious traps for hydrogen at lower temperatures, may improve the susceptibility to HE. Additionally, vanadium and niobium dissolving in austenite may induce a certain amount of strengthening by solute drag. Intercritical annealing at a temperature above 850 °C yields a microstructure richer in martensite which has previously been shown to be most susceptible to HE [19, 37].

The variation of elongation at fracture with intercritical annealing temperature is illustrated in Fig. 18. Hydrogenation drastically reduces the percentage elongation at fracture for all temperatures. The material intercritically annealed at 740 °C displays a slightly higher elongation (2.5%) due to the presence of a higher proportion of ferrite present. Around 800 °C NbC and VC act as effective initiation sites for hydrogen-induced cracking, thus reducing the observed ductility. Between 800 and 850 °C carbide dissolution is one of the primary factors controlling the charged plasticity. Above 850 °C, the increasing volume fraction of martensite and retained austenite films exercise detrimental effects as discussed earlier. The fact that high-temperature austenitizing treatment decreases the tensile ductility with some reduction in strength is confirmed by the recent work of Cao and Lu [38]. Variations in the amount, distribution and mechanical stability of retained austenite, particularly the occurrence of an interlath austenite film, are singled out as being detrimental to the mechanical properties in question.

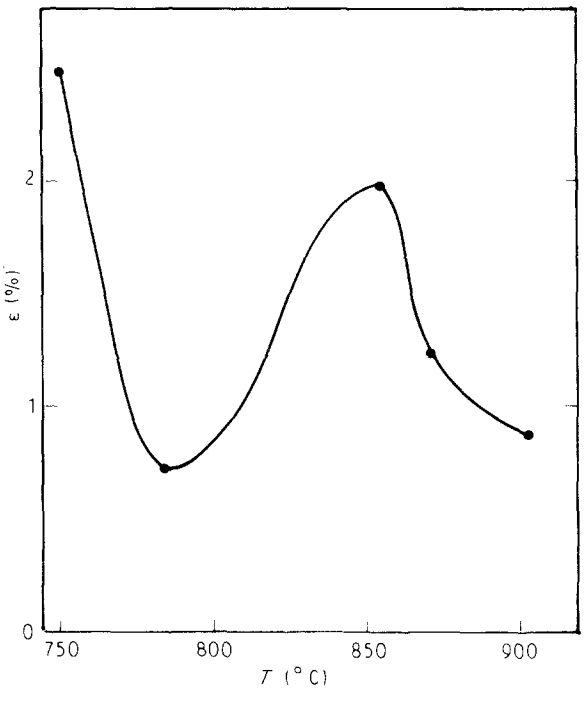

Figure 18 Variation of tensile ductility with intercritical annealing temperature for hydrogenated dual phase steel.

4. Discussion

Due to its low carbon content, the steel develops under equilibrium cooling conditions a predominantly ferrite matrix with a small amount of pearlite/carbide aggregates. The high fraction of ferrite (about 99%) accounts for the ductile fracture of this steel, which is shown to occur by microvoid coalescence. Hydrogenating the steel in the as-received condition results in an appreciable degradation of mechanical properties. This is attributed to build-up of internal hydrogen pockets in "injurious" sites within the microstructure, which upon exceeding a certain critical value are capable of inducing permanent damage in the form of cracks even in the absence of an externally applied stress. Thus, hydrogen asserts its influence in two ways. Firstly, it can reduce the effective cross-section of the material by generating internal and surface cracks. Secondly, internal hydrogen pressure is additive to the externally applied stress.

As the data deduced from stress–strain curves suggest, the enhancement of strength achieved by dual-phase heat-treatment is phenomenal. For instance, intercritical annealing at 749 °C followed by quenching imparts an additional 50% increase of UTS to the as-received steel. With increased ICT, the contribution to UTS and 2% flow stress becomes even more emphatic. The ductility, on the other hand, experiences a marked decline relative to that of the as-received material. Unlike the as-received material, the dual-phase steel is characterized by continuous yielding behaviour, a rapid rate of work-hardening but a relatively lower ductility than that observed with the as-received stock.

Regarding the possible causes of continuous yielding in dual-phase steel, various metallurgical factors such as the density of mobile dislocations, prior austenite grain size, ICT and the cooling rate following annealing have all been shown to have a different degree of influence on the yield behaviour. Additionally, the presence of a certain amount of pearlite in a ferrite–martensite matrix has been associated with discontinuous yielding but with no suggested rationale. However, the proposal that mobile dislocations

introduced during the austenite-to-martensite transformation [30] could account for continuous yielding in dual-phase steel appears to have gained wide acceptance. The combination of high residual stresses and a high mobile dislocation density in the ferrite causes plastic flow to take place easily at low plastic strains [39]. Consequently, yielding occurs at numerous sites throughout the ferrite and discontinuous yielding is suppressed [40].

In order to suppress discontinuous yielding the necessity of a minimum amount of martensite has been proposed [32]. The critical amount of martensite is reported to be in the range 5–15%. Hansen and Pradhan [41] report that at a cooling rate of 12 °C s^{-1} the yield strength goes through a minimum irrespective of chemical composition or annealing temperature. At this cooling rate a transition from discontinuous to continuous yielding is observed. Also a maximum is observed in the uniform elongation at this rate. Increasing the cooling rate and/or the annealing temperature increases the amount of martensite. In the present work the fast cooling rate (370–450 °C s^{-1}) from ICT resulted in a microstructure primarily consisting of ferrite and martensite with a small amount of retained austenite. No pearlite was detected in the equilibrium microstructure.

The dependence of 2% flow stress on the intercritical annealing temperature is presented in Fig. 19. The flow stress registers an impressive increase from 670 to 1109 MPa upon increasing the annealing temperature from 749 to 900 °C. This 65.5% increase is unequivocally related to the strengthening influence of dispersed martensite, which acts as an effective barrier to dislocation movement. The comparatively low flow stress observed around 800 °C is thought to be due to retained austenite, and partial dissolution of VC carbide which exhibits a higher solubility in austenite than NbC at lower temperatures. Probably for the same reason, elongation at fracture passes through a peak around the same temperature. These observations are in agreement with the recent findings of Goel *et al.* [42] who reported that the austenite formed by intercritical annealing up to 792 °C, where the kinetics is dominated by higher nucleation rates, is more susceptible to retention than that formed beyond 792 °C, where the kinetics is primarily dominated by higher growth rates.

Similarly the UTS is sensitively dependent upon the ICT. As shown in Fig. 20, the UTS increases from 957 MPa (for ICT = 749 °C) to 1366 MPa (for ICT = 853 °C) at a rate of 438 MPa per 100 °C, and goes through a peak value at 870 °C after which it begins to decline relatively slowly to 1362 MPa for an ICT of 900 °C. An explanation is offered for these observations in terms of two conflicting trends. As the temperature of annealing increases, the volume fraction of martensite also increases. This results in strengthening. On the other hand, increasing the ICT reduces the driving force for the austenite-to-martensite transformation due to a lowering of the carbon content of austenite, thus causing some austenite retention and concomitant lowering of the strength. Alloying elements also greatly influence the amount of austenite retained upon quenching. For example, 1% vanadium in a 0.2% C steel quenched from 1150 °C can cause 5% martensite to be retained. The austenite, which occurs as a network of thin film around the martensite laths, is revealed as a fine network by employing dark-field electron microscopy using a gamma diffraction beam. Due to its very small volume fraction and unfavourable morphology, the thin film of retained austenite between martensite laths does not contribute to the ductility.

Variation of the percentage elongation at fracture of unhydrogenated dual-phase steel is demonstrated in Fig. 21. The ductility is seen to increase appreciably on increasing the ICT from 749 to 783 °C. Around 800 °C the ductility reaches a maximum. This is in conformity with the observation of a relative lowering in the 2% flow stress occurring around the same temperature, when dissolution of carbides of vanadium and niobium gives rise to enhanced ductility. For higher

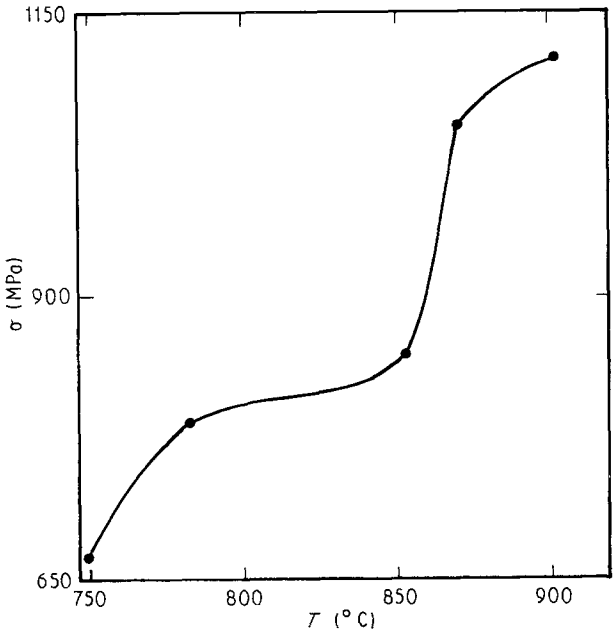

Figure 19 Variation of 2% flow stress with intercritical annealing temperature for uncharged dual-phase steel.

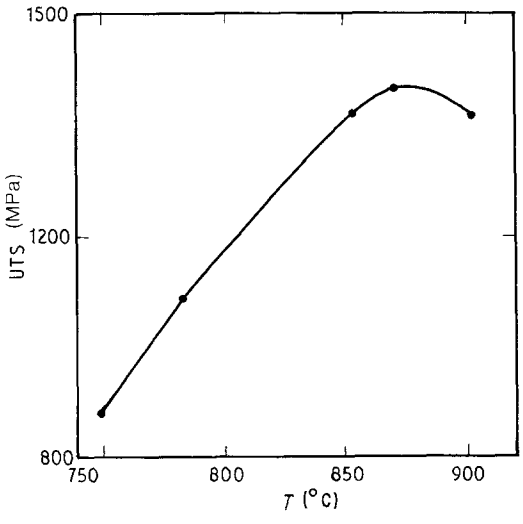

Figure 20 Variation of ultimate tensile strength (UTS) with intercritical annealing temperature for uncharged dual-phase steel.

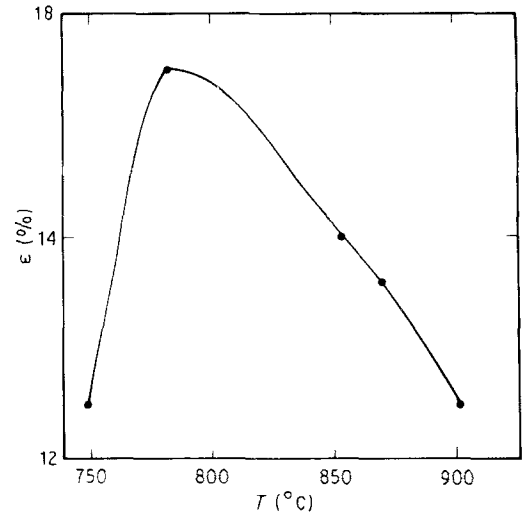

Figure 21 Variation of tensile ductility with intercritical annealing temperature for uncharged dual-phase steel.

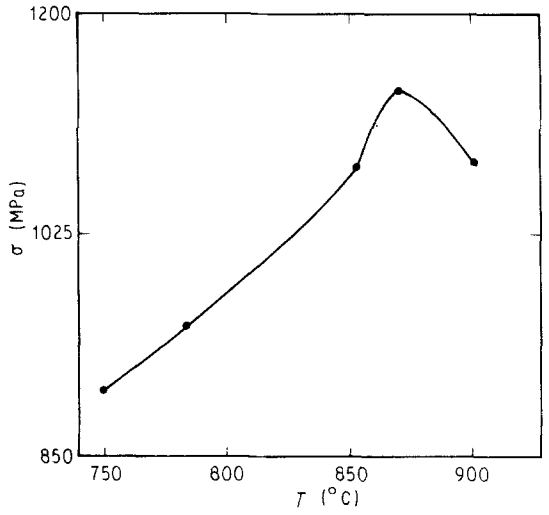

Figure 22 Variation of fracture strength with intercritical annealing temperature for uncharged dual-phase steel.

ICTs, however, the progressive increase in the volume fraction of martensite and the change in its morphology become preponderant so that the ductility is consistently lowered.

The trend observed in the dependence of flow stress and UTS on the ICT is generally valid in the variation of the fracture strength with ICT. As Fig. 22 depicts, the fracture strength increases steadily with increasing ICT up to 870 °C. Henceforth, the fracture strength falls with increasing ICT. The increase in the fracture strength is related to an increasing volume fraction of martensite, while the fall in strength is attributed to the deleterious influence of retained austenite films between martensitic laths.

5. Conclusions

1. The dual-phase microstructure has been shown to be much more susceptible to HE than the ferrite–pearlite microstructure.

2. Residual stresses arising from the austenite-to-martensite transformation promote cleavage and intergranular fracture as well as hydrogen-induced cracking (HIC) on flat surfaces.

3. Retained austenite transforming to martensite reduces the ductility in both uncharged and charged specimens.

4. At relatively low temperature (below 800 °C), carbides of niobium and vanadium act as damaging traps and enhance HE.

5. An adequate heat treatment to relieve internal stresses may reduce susceptibility to HE.

Acknowledgement

The authors would like to thank King Abdulaziz University Research Directorate for the financial support of this research (Project No. 407-079).

References

1. H. NORBERG and B. ARONSSON, *J. Iron Steel Inst.* **206** (1968) 1263.
2. K. NARITA, *Trans. Iron Steel Inst. Jpn* **15** (1975) 147.
3. G. L. DUNLOP and P. J. TURNER, *Met. Sci.* **9** (1975) 370.
4. D. C. HOUGHTON, G. C. WEATHERBY and J. D. EMBURY, in "Thermomechanical Processing of Microalloyed Austenite", edited by A. J. De Ardo, G. A. Ratz and P. J. Wang (Metals Society, AIME, Warrendale, 1982) p. 267.
5. N. K. BALLIGER and R. W. K. HONEYCOMBE, *Met. Sci.* **14** (1980) 121.
6. G. L. DUNLOP and R. W. K. HONEYCOMBE, *ibid.* **14** (1980) 367.
7. T. GLADMAN, *Proc. R. Soc.* **294** (1966) 298.
8. *Idem.*, in "Recrystallization and Grain Growth of Multi-Phase and Particle Containing Materials", edited by N. Hansen, A. R. Jones and T. Leffers (Riso National Laboratory, Riso, Denmark, 1980) p. 183.
9. C. J. TWEED, N. HANSEN and B. RALPH, *Met. Trans.* **14A** (1983) 2235.
10. W. B. MORRISON and J. H. WOODHEAD, *J. Iron Steel Inst.* **201** (1963) 43.
11. A. T. DAVENPORT, F. G. BERRY and R. W. K. HONEYCOMBE, *Met. Sci.* **2** (1968) 104.
12. F. G. BERRY and R. W. K. HONEYCOMBE, *Met. Trans.* **1** (1970) 3279.
13. R. W. K. HONEYCOMBE, in "Phase Transformation in Ferrous Alloys", edited by A. R. Marder and J. I. Goldstein, (Metals Society, AIME, 1984) p. 259.
14. J. M. GRAY, T. KO, ZHANG SHOUHAU, WU BAORONG and XIE XISHAN (eds), "HSLA Steels, Metallurgy and Applications", Proceedings of International Conference, November 1985, Beijing (ASM, Ohio, 1986).
15. A. J. DE ARDO (ed.), "Processing, Microstructure and Properties of HSLA Steels", Proceedings of International Symposium, November 1987, Pittsburg, Pennsylvania (Minerals, Metals and Materials Society, Warrendale, 1988).
16. I. M. BERNSTEIN, R. GARBER and G. M. PRESSOUYRE, in "Effects of Hydrogen on Behaviour of Materials", edited by A. W. Thompson and I. M. Bernstein (TMS, New York, 1976) p. 27.
17. D. A. RYDER, T. GRUNDY and T. J. DAVIES, in Proceedings of 1st International Conference on Current Solutions to Hydrogen Problems in Steels, Washington, DC, November 1982, edited by C. G. Interrante and G. M. Pressouyre (ASM, Metals Park, 1982) p. 272.
18. P. LACOMBE, M. AUCOUTURIER and J. CHENE, in "Hydrogen Embrittlement and Stress Corrosion Cracking", edited by R. Gibala and R. F. Hehemann (ASTM, Metals Park, 1984) p. 79.
19. T. ALP, B. DOGAN and T. J. DAVIES, *J. Mater. Sci.* **22** (1987) 2105.
20. A. McNABB and P. K. FOSTER, *Trans. Met. Soc. AIME* **227** (1963) 618.

21. H. H. JOHNSON and R. W. LIN, in "Hydrogen Effects in Metals", Proceedings of 3rd International Conference on Effects of Hydrogen on Behaviour of Materials, Wyoming, August 1980, edited by I. M. Bernstein and A. W. Thompson (Metallurgical Society of AIME, Warrendale, 1981) p. 3.
22. R. A. ORIANI, *Acta Metall.* **18** (1970) 147.
23. R. GIBALA, in "Stress Corrosion Cracking and Hydrogen Embrittlement of Iron Base Alloys", edited by R. W. Staehle, J. Hochmann, R. D. McCright and J. E. Slater (NACE, Houston, 1977) p. 244.
24. J. P. HIRTH, *Met. Trans.* **11A** (1980) 861.
25. B. B. RATH and I. M. BERNSTEIN, *Met. Trans. A* **2** (1971) 2845.
26. G. M. PRESSOUYRE, PhD thesis, Carnegie-Mellon University (1977).
27. G. M. PRESSOUYRE and I. M. BERNSTEIN, *Corrosion Sci.* **18** (1978) 819.
28. G. M. PRESSOUYRE, *Acta Metall.* **28** (1980) 1980.
29. S. HAYAMI and T. FURUKAWA, in Proceedings, "Microalloying 75", London, Session 2A (Vanitec, London, 1975) p. 78.
30. M. S. RASHED, "A Unique High-Strength Sheet Steel with Superior Formability", SAE reprint 760206 (1976).
31. R. A. KOT and J. W. MORRIS (eds), "Structure and Properties of Dual-Phase Steels" (AIME, New York, 1979).
32. J. M. RIGSBEE and P. J. VANDERAREND, in "Formable HSLA and Dual-Phase Steels", edited by A. T. Davenport (AIME, New York, 1979).
33. R. A. ORIANI, *Ann. Rev. Mater. Sci.* **8** (1978) 327.
34. I. M. BERNSTEIN and A. W. THOMPSON, in "Hydrogen Embrittlement and Stress Corrosion Cracking", edited by R. Gibala and R. F. Rehemann (ASM, Ohio, 1984) p. 135.
35. J. H. WOODHEAD, "Vanadium in High Strength Steels" (Vanitec, London, 1979) p. 3.
36. K. J. IRVINE, F. B. PICKERING and T. GLADMAN, *J. Iron Steel Inst.* **205** (1967) 161.
37. A. W. THOMPSON and I. M. BERNSTEIN, *Adv. Corros. Sci. Technol.* **7** (1980) 53.
38. W. CAO and X.-P. LU, *Met. Trans.* **18** (1987) 1569.
39. D. K. MATLOCK, G. KRAUSS, L. RAMOS and G. S. HUPPI, in "Structure and Properties of Dual-Phase Steels", edited by R. A. Kot and J. W. Morris (AIME, New York, 1979) p. 62.
40. G. R. SPEICH, in "Metals Handbook", Vol. 1, 10th Edn (ASM, Ohio, 1990) p. 424.
41. S. S. HANSEN and R. R. PRADHAN, in "Structure and Properties of Dual-Phase Steels" edited by R. A. Kot and J. W. Morris (AIME, New York, 1979) p. 113.
42. N. C. GOEL, J. P. CHAKRAVARTY and K. TANGRI, *Met. Trans. A* **18** (1987) 5.

Received 23 July 1990
and accepted 6 February 1991